Fermi National Accelerator Laboratory

FERMILAB-Pub-76/42-EXP
7300.358

(Submitted to Phys. Rev. Lett.)

DYNAMICS OF INCLUSIVE DIMUON PRODUCTION

M. Binkley, I. Gaines, J. Peoples, B. Knapp, W. Lee,
P. Leung, S. D. Smith, A. Wijangco, J. Knauer,
J. Bronstein, R. Coleman, G. Gladding, M. Goodman,
M. Gormley, R. Messner, T. O'Halloran,
J. Sarracino, and A. Wattenberg
Fermi National Accelerator Laboratory, Batavia, Illinois 60510
Columbia University, Irvington on Hudson, New York 10533
University of Hawaii, Honolulu, Hawaii 96822
University of Illinois, Urbana, Illinois 61801

May 1976

DYNAMICS OF INCLUSIVE DIMUON PRODUCTION

M. Binkley, I. Gaines, J. Peoples, B. Knapp, W. Lee,
P. Leung, S. D. Smith, A. Wijangco, J. Knauer,
J. Bronstein, R. Coleman, G. Gladding, M. Goodman,
M. Gormley, R. Messner, T. O'Halloran,
J. Sarracino, and A. Wattenberg
Fermi National Accelerator Laboratory, Batavia, Illinois 60510
Columbia University, Irvington on Hudson, New York 10533*
University of Hawaii, Honolulu, Hawaii 96822*
University of Illinois, Urbana, Illinois 61801†

ABSTRACT

We have measured the $p_\perp$ and $p_\parallel$ dependence of J production by high energy neutrons in comparison with the production of the conventional vector mesons. We also report values for total inclusive cross sections for resonance and continuum dimuons, and give an upper limit for ψ' production.

*Supported by the National Science Foundation.

†Supported by the United States Energy Research and Development Administration.

Although it has been a year and a half since the discovery of J[1,2] and of the ψ' (3684) particles,[3] very little is known about the mechanism for their production by hadrons. The increase of the inclusive cross section for J production by a factor of one hundred between 30 GeV and 300 GeV does not have an experimentally verifiable explanation.[4] We have made a measurement of the dynamical dependence of this inclusive cross section. At the same time we have measured the same properties of the inclusive cross sections for ρ, ω, and ϕ production in order to compare these data with the J data. In addition, we have measured the production dynamics of dileptons of masses between the ϕ and the J in order to determine whether the dominant source of these dileptons is a Drell-Yan continuum of virtual photons.

Our results were obtained from an analysis of dimuon production by 300 GeV neutrons[5] on nuclear targets in a high energy neutron beam at Fermilab. The A-dependence of the dimuon cross section was reported in Ref. 5, where we also described the apparatus and the methods of analysis.

The data was divided into five mass regions: $\rho + \omega$, .6 to .9 GeV/c^2; ϕ, .9 to 1.15 GeV/c^2; C_1 (continuum), 1.15 to 1.4 GeV/c^2; C_2 (continuum), 1.4 to 2.6 GeV/c^2; and J , 2.6 to 3.6 GeV/c^2. The calculation of yields and background subtractions has been described in Ref. 5. Background corrections were only necessary in the first three mass regions. The yields from all targets were summed to give the $p_\perp$ and $p_\parallel$ distributions shown in Fig. 1 and 2 and fitted as described below.

We parameterized the invariant cross section for inclusive dimuon production in each mass interval by:

$$E\frac{d^3\sigma}{dp^3} = C(M)(1 - X_F)^{\alpha(M)}\ e^{-b(M)p_\perp} \qquad X_o < X_F < 1$$

$$E\frac{d^3\sigma}{dp^3} = C'(M)\ e^{-b(M)p_\perp}\ 0 < X_F < X_o \qquad C' = C(1 - X_o)^{\alpha} \tag{1}$$

The actual yield of dimuons as a function of $p_\perp$ and X_F[6] was compared to the yield of events generated by a Monte-Carlo calculation in order to determine values for the parameters α, b, and X_o in each mass interval. Equation 1 was used to determine the probability of producing a dimuon as a function of $p_\perp$ and X_F. The laboratory momentum for the Monte-Carlo generated events was computed using an incident neutron momentum distribution given by:[7]

$$\frac{dN}{dE} = \frac{E}{400} \qquad 0 < E < 320$$

$$\frac{dN}{dE} = 4\left(1 - \frac{E}{400}\right) \qquad 320 < E < 400 \tag{2}$$

The calculation included the effects of multiple scattering, ionization loss, and straggling in the absorber, the limiting of the acceptance by the finite apertures of the magnet and MWPC's, and the effect of the finite resolution of the MWPC's. Finally, we assumed that the angular distribution of the positive muon was isotropic in the dimuon center of mass.

The parameters α, b, and X_o were varied until the difference in shape between the Monte-Carlo sample of events and the data was a minimum. The $p_\perp$ and $p_{||}$ distributions for the $\rho + \omega$ and the J mass regions together with the best fit Monte-Carlo distributions are shown in figures 1 and 2. The efficiency for detecting a dimuon with $X_F < .2$ was greater than 10% only in the $\rho + \omega$ mass region, as can be seen from the dotted curves in Fig. 2. The value of $X_o = 0.3$ determined from the $\rho + \omega$ region was used in the fits for all masses.

The results of these calculations are given in Table I. The use of more refined models for the cross section and the neutron spectrum did not significantly improve the quality of the fits of the Monte-Carlo distribution to the data. However, the value of α was sensitive to the value of the energy at which the neutron spectrum peaks. Changing this peak energy from 320 GeV by ± 10% changes the value of α by 1/2 unit.

While we assumed an isotropic angular distribution for the decay, there was sufficient data in the $\rho + \omega$ mass region to test this assumption. Figure 3 shows the observed distributions in dimuon energy asymmetry ($|E_+-E_-/E_++E_-|$), compared to Monte-Carlo generated distributions for the three hypotheses of $1 + \cos^2\theta$, isotropic, and $\sin^2\theta$. The results clearly favor an isotropic distribution.

These values of $\alpha(m)$ are within the range of values which have been observed for hadrons. For example, Taylor et al.,[8] have found that π's and K's have a value of α between 2 and 4

while $\bar{p}$'s have $\alpha \simeq 8$. It is worth noting that our data show that the ρ inclusive cross section is independent of X_F for $X_F < .3$.

The parameter b which characterizes the $p_\perp$ distribution decreases monotonically as the mass of the dimuon increases. We point out that the value of b at the J mass is not due to an unreliable extrapolation since we have observed J's produced with $p_\perp > 3$ GeV/c. Furthermore, a parameterization which is proportional to $e^{-b*p_\perp^2}$ is inconsistent with our data.

The total integrated inclusive cross section for dimuon production for $X_F > 0.24$ in each mass interval was determined from the yield of events normalized to the incident neutron flux, as described in Ref. 5, and the geometric efficiency as determined from the Monte-Carlo calculation. The cross sections were extrapolated to A = 1 using the A-dependences measured in Ref. 5. These results are given in Table I.

In the ϕ mass region, we assumed the same A dependence as in the $\rho+\omega$ region. No subtraction was made for the $\rho+\omega$ tail, so the values of α, b, and the cross section are for all dimuons in the ϕ mass region. We estimate that between 1/2 and 2/3 of the cross section is due to the ϕ.

Since there was reasonable acceptance for $X_F < 0.24$ in the $\rho+\omega$ mass interval, a total inclusive cross section could be determined. We find that $B^\rho_{\mu\mu} \cdot \sigma^\rho + B^\omega_{\mu\mu} \cdot \sigma^\omega = 700$ nb/nucleon. We can then determine σ^ρ for two extreme assumptions about the amount of ω production:[9]

$$\sigma^\rho = 16 \text{ mb if } \sigma^\omega = 0, \text{ and}$$

$$\sigma^\rho = 6 \text{ mb if } \sigma^\rho = \sigma^\omega \ .$$

The best fit to the mass spectrum requires some ω production. The second result is consistent with the value of 6 mb for inclusive ρ^o production in 205 GeV pp collisions.[10] That experiment detected the ρ through its 2π decay mode.

The integrated inclusive cross section for J for $X_F > 0.24$ is in agreement with previous experiments.[11] Assuming that $d\sigma/dy$ is constant for $0 < X_F < 0.3$ (y = center of mass rapidity) we obtain

$$B^J_{\mu\mu} \left.\frac{d\sigma}{dy}\right|_{y=0} = 8.9 \text{ nb per nucleon,}$$

which agrees well with the recent measurement of Snyder et al.[13] Such a flattening at low X_F has been observed in other measurements of J production[12] as well as in the measurements of the ρ presented here. If one uses this extrapolation for the unobserved region of X_F the total inclusive cross section is $B^J_{\mu\mu}\sigma^J_{tot} = 22$ nb per nucleon.

We have studied the events with mass above 3.5 GeV/c^2 for evidence of ψ' (3684) production. The 12 events from the data in the mass range 3.5 - 3.9 GeV/c^2 are equal to a predicted 12 events in this range due to the tail of the J. Since we have no evidence for ψ' production, we place a 90% confidence level upper limit for ψ' production in our kinematic range of $X_F > .25$ of

$$R = \frac{B^{\psi'}_{\mu\mu} \cdot \sigma^{\psi'}}{B^J_{\mu\mu} \cdot \sigma^J} < .015 \qquad 90\% \text{ C. L.}$$

Snyder et al.[13] have recently measured this ratio to be $.014 \pm .004$ at $X_F = 0$.

The value of $\frac{d\sigma}{dM^2}$ per nucleon is shown plotted in Fig. 4. We have calculated the expected yield of Drell-Yan pairs for

$P_{||} > 75$ GeV under two assumptions for νW_2[14] and these are shown as solid and dashed curves in Fig. 4. We have assumed three colors in each case. The observed yield is greater than the predictions.

In conclusion, we find that the dynamical dependence of inclusive dimuon production does vary with dimuon mass, but that there seem to be no differences between ρ and J production which cannot be attributed to the heavier mass of the J.

REFERENCES

[1]J. J. Aubert, et al., Phys. Rev. Lett. 33, 1404 (1974).

[2]J. E. Augustin, et al., Phys. Rev. Lett. 33, 1406 (1974).

[3]G. S. Abrams, et al., Phys. Rev. Lett. 33, 1453 (1974).

[4]B. Knapp, et al., Phys. Rev. Lett. 34, 1044 (1975).

F. W. Busser, et al., Phys. Lett. 56B, 482 (1975).

G. J. Blanar, et al., Phys. Rev. Lett. 35, 346 (1975).

K. J. Anderson, et al., Phys. Rev. Lett. 36, 237 (1975).

[5]Previous letter.

[6]X_F is the ratio of p to p_{max} in the neutron-nucleon center of mass system. If we had chosen the alternate parameterization $\frac{d\sigma}{dx} = C(1-x)^{\alpha^*}$, then $\alpha^* \simeq \alpha + 1.5$.

[7]T. Ferbel, in Proceedings of the International School of Subnuclear Physics, "Ettore Majorana", Erice, 1975, edited by A. Zichichi (Academic, New York, 1976).

M. Longo, et al., University of Michigan Report No. UM-HE-74-18 (unpublished).

[8]F. E. Taylor, et al., Fermilab-PUB-75/90 EXP (1975), submitted to Phys. Rev. D.

[9]We have used branching ratios for the ρ and ω dilepton decays of $B^{\rho}_{\mu\mu} = 4.3 \times 10^{-5}$ and $B^{\omega}_{\mu\mu} = 7.6 \times 10^{-5}$, as determined from storage ring measurements: Particle Data Group, Review of Particle Properties, Rev. Mod. Phys. 48, 51 (1976).

[10] R. Singer, et al., Phys. Lett. 60B, 385 (1976).

[11]We note several important systematic effects on the absolute cross section. If the J angular decay distribution is $1 + \cos^2\theta$ rather than isotropic, the cross section is raised by 30%. In addition, uncertainties in the incident neutron spectrum introduce an uncertainty in all absolute cross sections of ±25%.

[12]Y. M. Antipov et al., Phys. Lett. 60B, 309 (1976).

K. J. Anderson, et al., Phys. Rev. Lett. 36, 237 (1975).

[13]H. D. Snyder, et al., Fermilab-PUB-76/32 EXP.

[14]The calculation was made using alternate sets of parton distribution functions:

R. Blackenbecler, et al., SLAC-PUB-1531 (1975), unpublished.

J. Okada, et al., University of Hawaii preprint UH-511-209-76 (1976).

In our kinematic range, the most important difference in these models is in the value of νW_2 (0).

TABLE I

PARAMETERS DESCRIBING INCLUSIVE DIMUON PRODUCTION

mass range	α	b	$.24\int_{}^{1.0} B_{\mu\mu} \frac{d\sigma}{dX_F} dX_F$ nanobarns/nucleon
$\rho+\omega$	3.0 ± 0.3	4.2 ± 0.2	100
ϕ	3.4 ± 0.6	3.5 ± 0.3	16.1
C_1	2.7 ± 0.8	3.5 ± 0.4	1.4
C_2	3.3 ± 0.5	2.4 ± 0.2	1.1
J	5.2 ± 0.5	1.6 ± 0.2	3.5

α, b described in text.

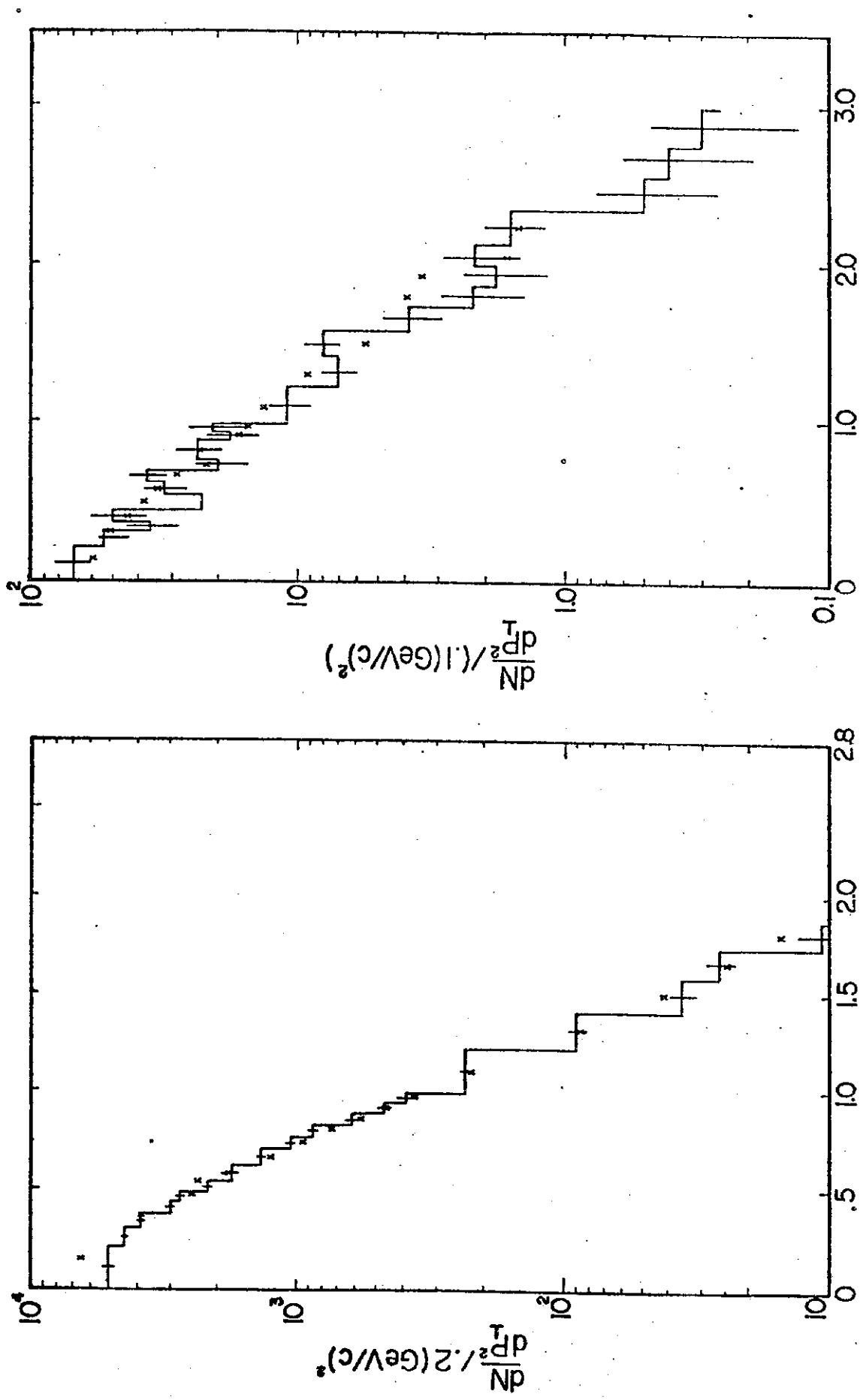

Fig. 1. $dN/dp_\perp^2$ vs. $p_\perp$. for a) $\rho + \omega$, b) J/ψ. Solid curve = raw data. x's = Monte Carlo calculation: $e^{-4.2p_\perp}$ for $\rho + \omega$

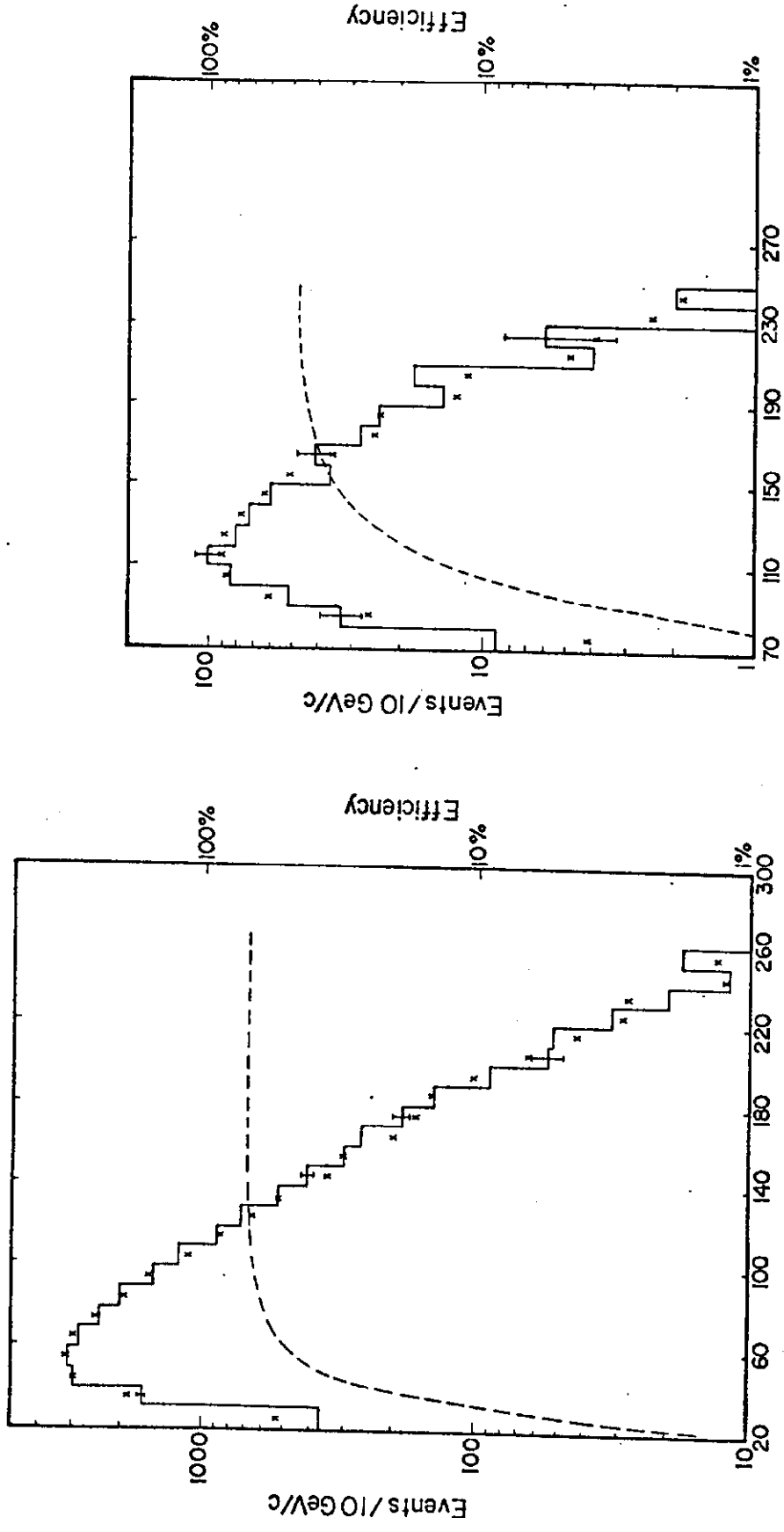

Fig. 2. dN/dp vs. $p_{||}$ for a) $\rho + \omega$, b) J/ψ. Solid curve = raw data. x's = Monte Carlo calculation, fits described in text. Dashed curve = efficiency.

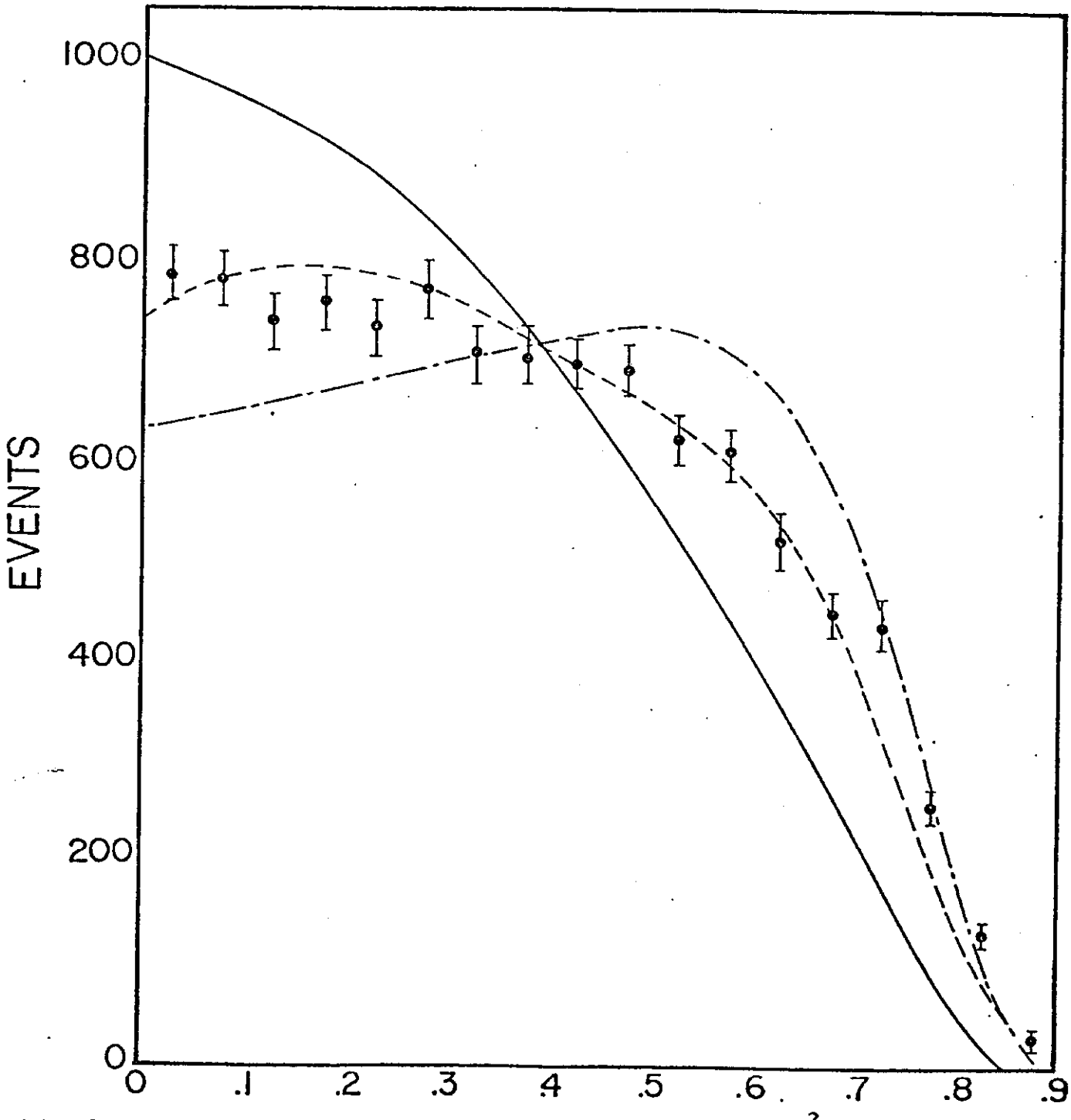

Fig. 3. Decay angular distribution for $\rho + \omega$. Solid line = $\sin^2\theta$ distribution. Dashed line = isotropic distribution. Dotted-dashed line = $1 + \cos^2\theta$ distribution.

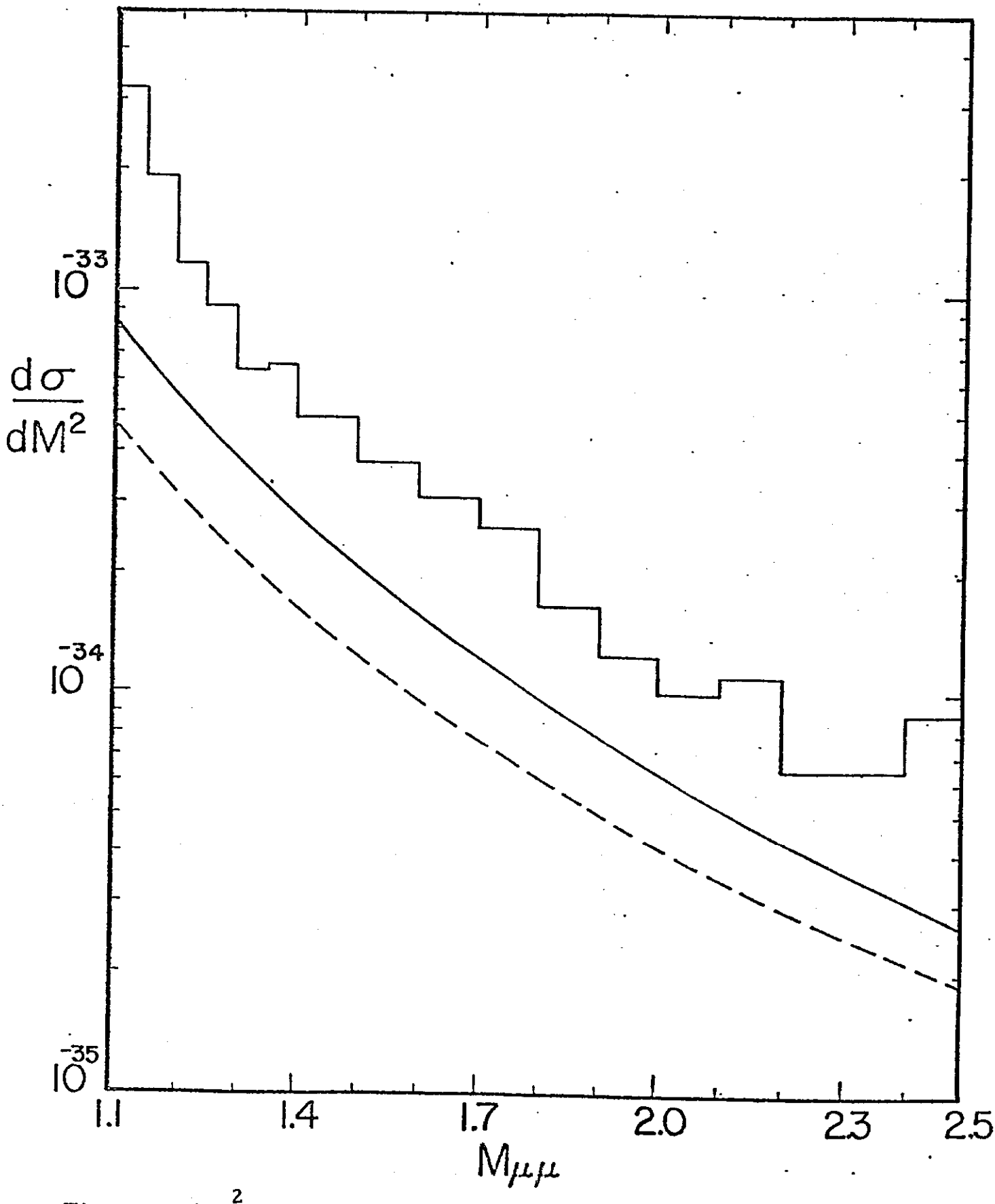

Fig. 4. $d\sigma/dM^2$ vs. M in continuum region, for $P_{\parallel} > 75$ GeV. Solid and dashed lines are Drell-Yan calculations with color included (Ref. 14).